Heliyon 10 (2024) e29458

Contents lists available at ScienceDirect

Heliyon

journal homepage: www.cell.com/heliyon

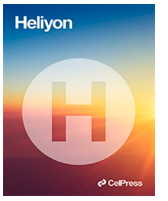

Research article

In vivo treatment of zinc phosphide poisoning by administration of mesoporous silica nanoparticles as an effective antidote agent

Fatemeh Farjadian [a,*], Reza Heidari [a], Soliman Mohammadi-Samani [a,b]

[a] *Pharmaceutical Sciences Research Center, School of Pharmacy, Shiraz University of Medical Sciences, Shiraz, Iran*
[b] *Department of Pharmaceutics, School of Pharmacy, Shiraz University of Medical Sciences, Shiraz, Iran*

ARTICLE INFO

Keywords:
Phosphine poisoning
Zinc phosphide
Antidote
Mesoporous silica nanoparticle
Rice tablet
Boric acid
Aluminium phosphide

ABSTRACT

Mesoporous silica nanoparticles (MSNs) are highly advanced engineered particles with increased surface area and extreme adsorption capacity for various molecules. Herein, two types of MSNs were synthesized and applied as adsorbents for phosphine gas. One was without functional groups (MSN), and the other was post-modified with boric acid (MSN-BA). The structures of MSN and boric acid-modified MSN with high surface areas of about 1025 and 650 m^2/g, respectively, were defined. MSN was found to have particles with sizes around 30 nm by transmission electron microscopy (TEM). In the present study, MSNs were used as an antidote to phosphorus poisoning, and zinc phosphide (phosphorus) powder was used as the toxic and lethal agent. *In vivo* analysis was carried out on rats to demonstrate the ability of MSNs to chemisorb phosphine gas. In the survival percentage assessment, Phos-poisoned animals were kept alive after treatment with MSNs, and the MSN-BA-treated group (dose of 5 mg/kg) was shown to have a 60 % survival rate. Blood serum analysis showed that MSNs have a high potential to alleviate organ blood damage, and serum biomarkers dropped sharply while phosphine-poisoned animals were treated with MSN-BA.

1. Introduction

One of the growing areas of nanotechnology is nanomedicine. It offers excellent solutions to obstacles in pharmaceutical science and the clinic: by recruiting nanoparticles, and new drug formulations with greater therapeutic efficacy and fewer side effects [1]. Several types of nanoparticles made of different materials, including polymers [2], graphene and graphene oxide [3], metallic [4], and silica [5], have been created and used for pharmaceutical purposes. Particles with higher surface areas have maximum adsorption capacity, and MSNs are a distinctive material with well-ordered porosity and high surface area. These materials are produced by using surfactants as directing agents. MCM-41 is one of the most widely used types of MSNs, prepared using cetyltrimethylammonium bromide (CTAB) as the directing agent. After the removal of CTAB, well-defined pores appear [5], and surface functionalization by post-modification is possible [6]. Mesoporous silica has a wide range of applications including in catalysis [7], wastewater purification [8,9], solid-phase extraction [10,11], sensors [12] and pharmaceuticals [13]. The masterpiece of MSN applications is in drug delivery, which can provide a unique platform for the loading and release of therapeutic agents [14] and is sometimes used for theranostic purposes [15–17].

On the other hand, MSNs have been defined as excellent candidates for the adsorption of metals and drugs [18,19]. These

* Corresponding author.
E-mail address: farjadian_f@sums.ac.ir (F. Farjadian).

https://doi.org/10.1016/j.heliyon.2024.e29458
Received 4 September 2023; Received in revised form 6 April 2024; Accepted 8 April 2024
Available online 16 April 2024

capabilities have been invoked in the design of antidotes for certain toxins, and the term was introduced by Farjadian et al. in 2015. Paracetamol and phenobarbital were adsorbed onto MSNs and showed greater adsorption affinity than activated charcoal, which is an effective antidote for several poisonings [20]. In this way, several *in vivo* experiments were carried out to demonstrate the potential of using MSN as an antidote for various toxins. Ethylenediaminetetraacetic acid-modified MSN was an effective iron and copper adsorbent when administered successfully in metal-induced toxicities [21,22].

In addition, succinic acid-substituted MS acted as an ammonia adsorbent and was used to treat hepatic encephalopathy [23]. Other researchers have also administered thiol-modified MS as an adsorbent for mercury in an animal model [24] and for the treatment of liver toxicity and iron-induced oxidative stress [25].

Aluminum phosphide (ALP) or zinc phosphide (Phos), known as rice tablets in Iran, is commonly used to protect agricultural grains from insects and rodents [26]. These chemicals are highly toxic to humans and animals and can release phosphine gas (PH_3) when in contact with moisture. Inhalation of this gas can induce severe toxicity [27]. In some parts of Asia, including India, Iran, and Sri Lanka, these tablets can be either accidently ingested or abused for suicide [28]. Phosphine gas poisoning is reported to have a high mortality rate [29]. The lethal dose 50 (LD_{50}) of Phos in humans was reported to be 80 mg/kg and a toxic dose of 4–5 g intake [30]. In one case study, the fetal dose of aluminum phosphide poisoning was 150–500 mg/70 kg, with a mortality rate of 70–100 % [31]. However, the lethality of phosphine could be variable for different Phos and ALP due to their reactivity to acid and the amount of phosphine released in the body. Previous animal studies reported an LD_{50} of 40 mg/kg of phosphine in mice [22] and a single LD_{100} dose of 20 mg/kg of ALP in rats [32]. In the current study, a supra-lethal dose of ALP (40 mg/kg in rats) was used to ensure the antidotal effect of the investigated MSNs. As no definite antidote agent is introduced for the treatment of such toxicity, emergency supportive therapies are necessary as soon as possible at the referral toxicology centers of hospitals to rescue the affected patients. Some usual treatments are the administration of sodium bicarbonate, antioxidants (*e.g.*, vitamin C), N-acetylcysteine, and mitochondria-protecting agents (*e.g.*, dihydroxyacetone) [33,34]. Although these strategies could enhance patients' survival, there are no specific treatments for this complication.

Recently, Farjadian et al. repurposed sevelamer as an antidote to ALP and evaluated it in the *in vivo* experiments. Sevelamer administration in animal models poisoned with ALP could survive them and significantly reduce blood biomarkers of organ damage [35].

In continuation of our efforts in introducing MS as an antidote agent for several toxins [20,21,23,36], MSNs are utilized to treat Phos-induced toxicity. In this regard, two types of MSNs were prepared, one without a functional group (MSN) and one functionalized with boric acid (MSN-BA). Animal studies were conducted in 6 groups of Sprague-Dawley rats, divided into control, Phos-treated, Phos-treated with MSN, and Phos-treated with MSN-BA. Two sets of tests were performed: one set monitored survival; the other measured serum biochemistry and adenosine triphosphate (ATP) levels; the results were compared to assess the effect of MSNs in reducing Phos toxicity *in vivo*.

2. Experiments

2.1. Animals

Sprague Dawley (200–250 g) rats were obtained from the Animal Breeding Center of Shiraz University of Medical Sciences (SUMS). The animals were placed in a standard polystyrene cage in a lumbering bed at $23 \pm 2\ ^{\circ}C$ temperature and humidity of ≈40 %. Food and fresh water were available in their cage. The animals were treated following the instructions approved by the local ethics committee of SUMS in the project with this Ethical Code: IR.SUMS.REC.1395.S823.

3. Materials

Tetraethyl orthosilicate (TEOS) and CTAB were bought from Merck Chemical Company. (3-aminopropyl) triethoxy silane (APTES) and boric acid were obtained from Sigma-Aldrich. Solvents were prepared from Kimia Mavad, Iran. Zinc phosphide (Phos) was purchased from Sigma-Aldrich.

3.1. Instruments

Fourier transform infrared (FTIR) spectroscopy was carried out to determine the functional groups in the MSNs using the Bruker VERTEX70 instrument. X-ray diffraction (XRD) spectroscopy was used to determine the crystallinity pattern using MPD 3000 D8, an advanced Bruker, AXS instrument. The pore sizes of MSNs were measured by nitrogen adsorption and desorption techniques (Belsorp Mini II). Thermogravimetric analysis (TGA) (Mettler, Toledo) was used to determine the amount of boric acid in MSNs. A Zeiss instrument (EM10C-80 KV) was used for transmission electron microscopy (TEM). Scanning electron microscopy (SEM) was performed on a MIRA3 TESCAN instrument. Serum biochemistry was measured using existing commercial kits, Mindray BS-200® autoanalyzer, and Pars Azmun® (Tehran, Iran) standard kits to assess organ damage of serum markers.

4. Methods

4.1. Synthesis of mesoporous silica without functional group (MSN)

A controlled-sized technique synthesized mesoporous silica using our previous procedure [20]. First, CTAB (0.62 mmol) was dissolved in a deionized (DI) water solution of 0.5 M ammonia and stirred at 1500 rpm. Then, an ethanolic solution (20 ml) of TEOS (0.7 mmol) was added dropwise for 10 min to the stirring solution. After 2 h of mixing, another portion of an ethanolic solution (10 ml) of TEOS (1.3 mmol) was added similarly. Then mixing continued for 24h at 50 °C, 1500 rpm. Finally, the resulting product was acquired by centrifugation (3 × 10 min, 18,000 rpm) and purified by washing with DI water (× 1), ethanol (× 2), and acetone (× 1), then samples were dried in an oven at 50 °C overnight. The resulting powder was then admixed in an ethanol solution containing hydrochloric acid (2 ml HCL, 100 ml ethanol) and refluxed for 24 h to separate CTAB. Then, the synthesized sample was purified and dried the same way as in the previous step.

4.2. Synthesis of boron siloxane mesoporous silica (MSN-BA)

Boron siloxane was prepared by the reaction of MSN with boric acid. By this means, MSN (0.3 g) was reacted with boric acid (0.15 g) in DI water (50 ml) and refluxed for 20 h at 70 °C. The sintered glass filtered the mixture and washed it with DI water, ethanol (× 3), and acetone. The product was dried in an oven at 100 °C overnight.

4.3. In vivo animal study

Male Sprague-Dawley rats (n = 36) were used. The animals were categorized into six groups as follows (n = six animals/group): 1) control group (receiving 1 ml/kg olive oil orally), 2) Phos. -treated group received zinc phosphide orally, 40 mg/kg in olive oil, 3) this group received zinc phosphide orally, 40 mg/kg zinc phosphide in olive oil, plus MSN (1 mg/kg, gavage), 4) the group received zinc phosphide orally, 40 mg/kg in olive oil + MSN (5 mg/kg, gavage), 5) the group received zinc phosphide orally, 40 mg/kg Phos. in olive oil + MSN-BA (1 mg/kg, gavage), 6) the group received Phos. orally, 40 mg/kg phosphorus in olive oil + MSN-BA (5 mg/kg, gavage).

Two series of animals with described divisions were monitored for two kinds of assessment. The survival percent was evaluated in the first series of animals by recording the mortality rate for seven consecutive days. In the other groups, animals were anesthetized (24 h after Phos. poisoning) by thiopental 100 mg/kg, i.p., and blood samples were collected from the abdominal aorta, and transferred to standard tubes, and centrifuged (3000 g, 10 min, 4 °C) to obtain serum.

Blood samples were used to measure the markers of organ injury, including lactate dehydrogenase (LDH), alanine aminotransferase (ALT), aspartate aminotransferase (AST), and creatine kinase-myocardial band (CK) levels. Heart, brain, liver, and kidney tissue samples were also evaluated for ATP content.

4.4. Tissue ATP levels

A commercial kit (ENLITEN®, Promega) was used for the assessment of tissue ATP levels using a luminescence intensity assessment method [37,38]. Brain, heart, liver, and kidney samples (500 mg) were homogenized in a Tris-HCl buffer (5 ml of 40 mM solution, 4 °C). Then, 100 μl of trichloroacetic acid (0.3 % w: v) was added, mixed well, and incubated on ice (10 min). Then, samples were centrifuged (16000 *g*, 20 min, 4 °C), and the supernatant was collected to determine tissue ATP level. The luminescence intensity was determined at λ = 560 nm (FLUOstar Omega® plate reader, BMG Labtech, Germany) [37,39].

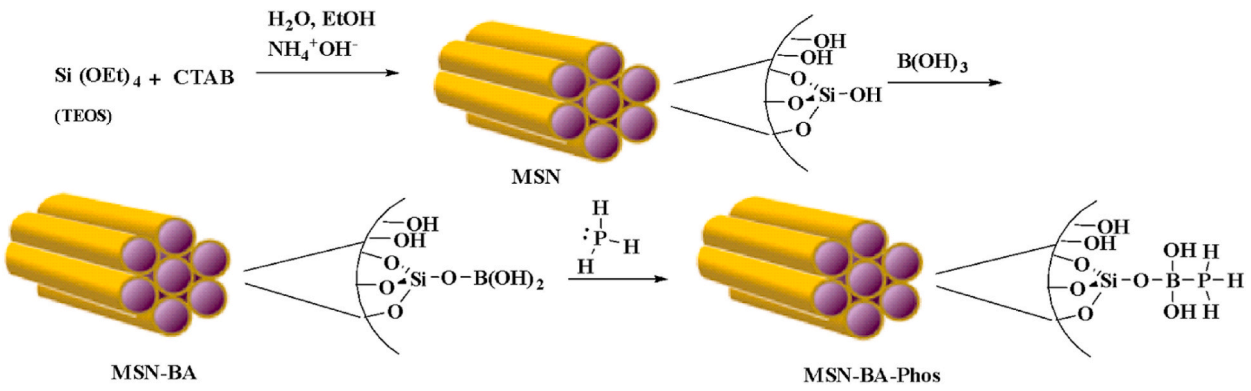

Fig. 1. Schematic illustration of the synthesis of MSN and MSN-BA.

4.5. Statistics

Data are presented as mean ± SD. One-way analysis of variance (ANOVA) with Tukey post hoc test was used to compare experimental groups. A $P < 0.05$ was considered a statistically significant difference.

5. Results

5.1. Synthesis and characterization of MSNs

In nanomedicine, mesoporous structured materials made of silica have received particular attention. In recent years, novel approaches have been introduced in the application of MS for managing toxicity in animal models [20–23]. In this context, two types of MSNs have been prepared, characterized, and used in animal models of phos-induced toxicity. The MSNs were prepared with the MCM-41 pattern following our previous size control technique and were used in animal models of Phos-induced toxicity [20]. The synthesis strategy of MSN and MSN-BA is depicted in Fig. 1. To synthesize MSN, TEOS was added to an aqueous medium of CTAB, and MSN was formed in a sol-gel process. For the preparation of borosilicate MSN (MSN-BA), the resulting product was then reacted with boric acid [40].

Boric acid is a weak Lewis acid with an empty p orbital, which can react with phosphine species with lone pair electrons [41]. As illustrated in Fig. 1, MSN-BA reacts with phosphine gas and produces MSN-BA-Phos. Boron reaches the octet rule in this reaction, and highly toxic phosphine gas can make an inert compound, MSN-BA-Phos.

FT-IR spectroscopy was carried out to define the functional groups in MSN and MSN-BA; the spectra are shown in Fig. 1. The results obtained on the structure of MSN confirm the presence of Si–O at 1130 cm^{-1} and Si–OH at 3400 cm^{-1} after the reaction of boric acid with MSN and its formation of MSN-BA, the new peaks appeared in the FTIR spectrum and the characteristic bands of Si-OB and B–O appeared at 609 cm^{-1} and 1862 cm^{-1} respectively (Fig. 2).

To determine the crystalline or amorphous nature of the MSN structure, two types of XRD spectroscopy, low angle and wide angle, were performed (Fig. 3A). Low angle XRD showed the characteristic band of MSN at 2.5° 2theta for the (*XYZ*) reflection of 100; the broad peaks around 10° and 25° could be due to the particles' small size and amorphous structure. Wide angle XRD spectroscopy was performed on MSN-BA, and the broad bands at 10° and 25° were representative of the amorphous group of SiO_2 in the structure; a small broad peak appeared at a 40–50° 2theta angle, as characteristic of boron oxide (Fig. 3B) [42].

TGA analysis of MSN and MSN-BA was carried out to determine the boron silicate content; at around 350 °C, MSN-BA showed a sharp decrease in weight loss, correlating with the oxidation of boron (Fig. 4A) [43]. The difference in weight loss percentage between MSN and MSN-BA is approximately 5 % in the B–O groups. An EDX analysis was carried out as further evidence for the determination of the boron density on MSN-BA, and it was found that boron has a weight of 31 % on MSN-BA (Fig. 4B).

To determine textural parameters such as surface area (m^2/g), pore size (nm), and pore volume (cm^3/g) of MSNs, N2 adsorption-desorption analysis was performed. Texture parameters are presented in Table 1; two methods, Barret-Joyner-Halenda (BJH) and Brunauer-Emmett-Teller (BET), extracted texture parameters from adsorption and desorption data. A large surface area of 1025 m^2/g was measured for MSN by BET, while for MSN-BA, this was reduced to 650 m^2/g due to pore occupancy with boric acid; comparing the results shows that MSN reacted successfully with boric acid. As a representative, the BET and BJH plots of the MSN-BA of N_2 adsorption/desorption are shown in Fig. 5. Herein, BET theory explains the physical adsorption of N_2 on the porous structure of MSN, and the plots showed the relationship between adsorbed gas and the amount of pressure, which resulted in the extraction of surface area data. Type II isotherm is observed for MSN-BA (Fig. 5A), demonstrating mono-layer N_2 adsorption at low and multilayer adsorption at medium pressure. BJH is a method for pore size calculation based on adsorption and desorption of N_2 gas at 77 K. BJH plot (Fig. 5B) shows the presence of meso-sized pores around 2 nm in the structure of MSN-BA.

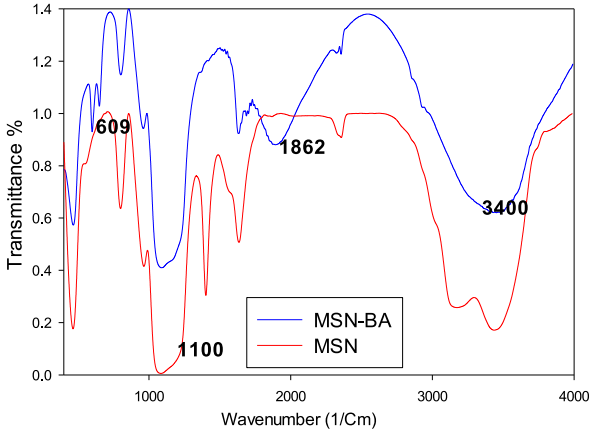

Fig. 2. FT-IR chromatograms of MSN and MSN-BA.

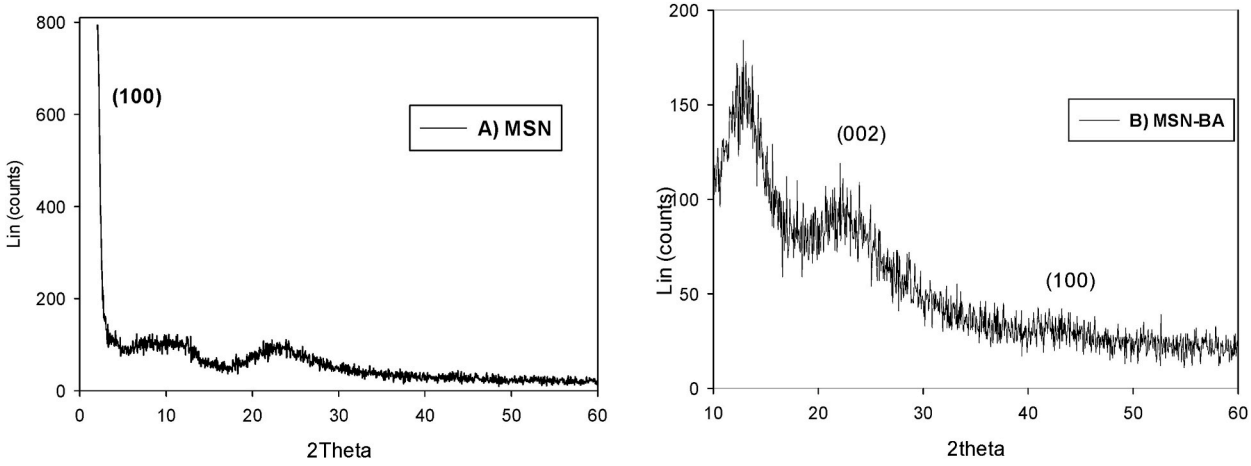

Fig. 3. XRD spectrum of A) MSN and B) MSN-BA.

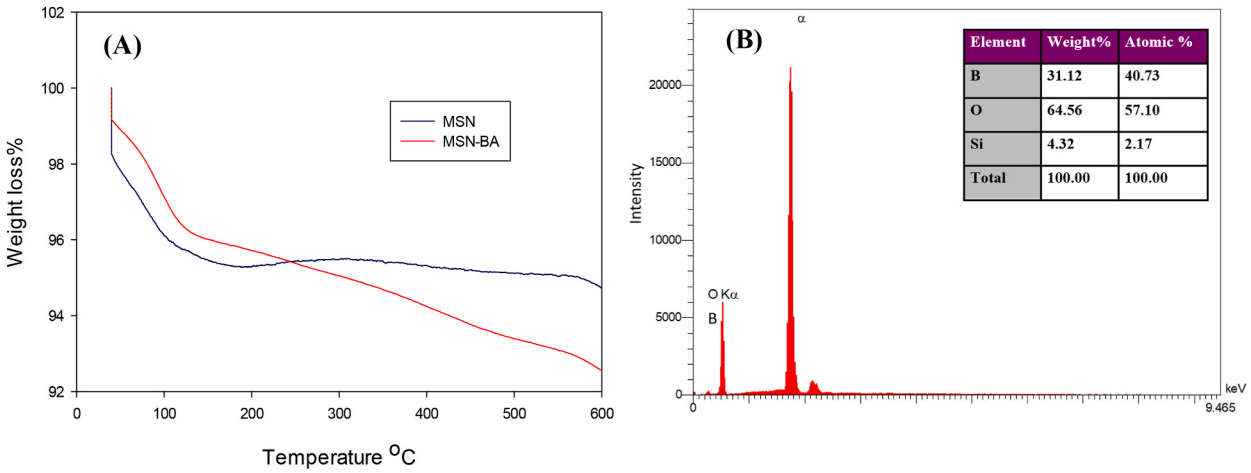

Element	Weight%	Atomic %
B	31.12	40.73
O	64.56	57.10
Si	4.32	2.17
Total	100.00	100.00

Fig. 4. (A) Thermograms of MSN and MSN-BA, and (B) EDX spectrum of MSN-BA and elemental percent Table.

Table 1
Textural BET and BJH parameters of MSN and MSN-BA.

Sample	BET method			BJH method		
	Surface area (m^2/g)	Total Pore volume (cm^3/g)	Pore diameter (nm)	Surface area (m^2/g)	Pore volume (cm^3/g)	Pore diameter (nm)
MSN	704.76	0.976	3.68	1025	1.54	2.97
MSN-BA	747.58	0.539	2.99	650.69	0.533	2.41

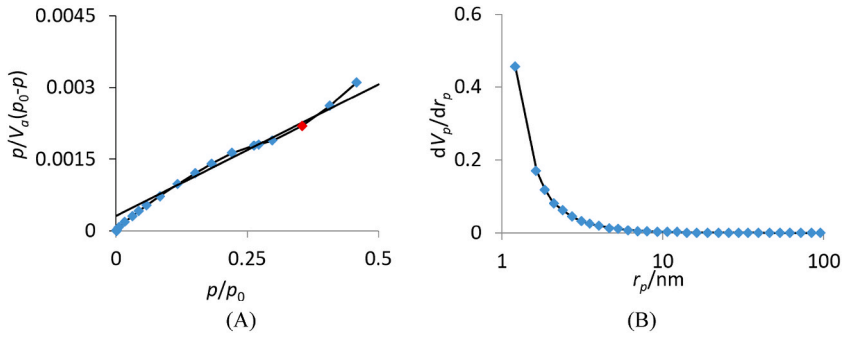

Fig. 5. (A) BET isotherm and (B) BJH pore size distribution plots of MSN-BA.

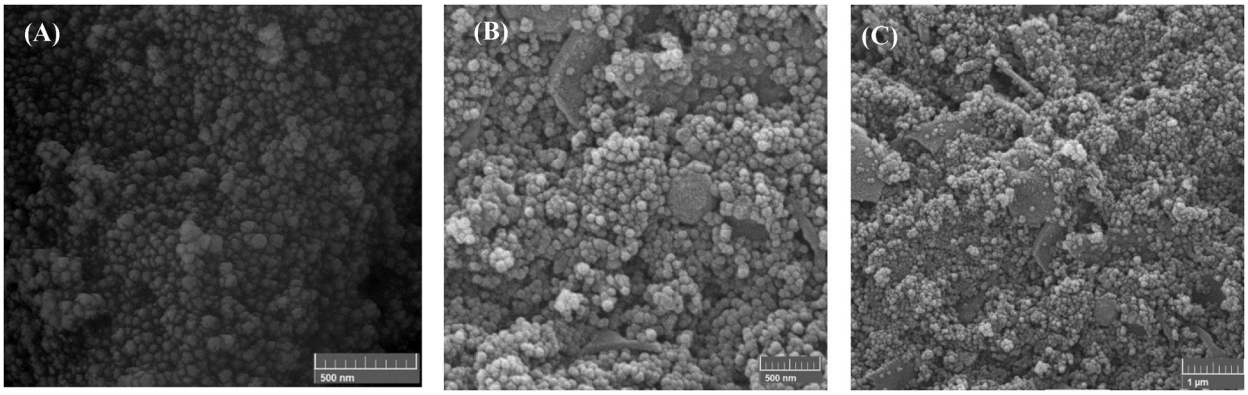

Fig. 6. SEM images of (A) MSN and (B&C) MSN-BA.

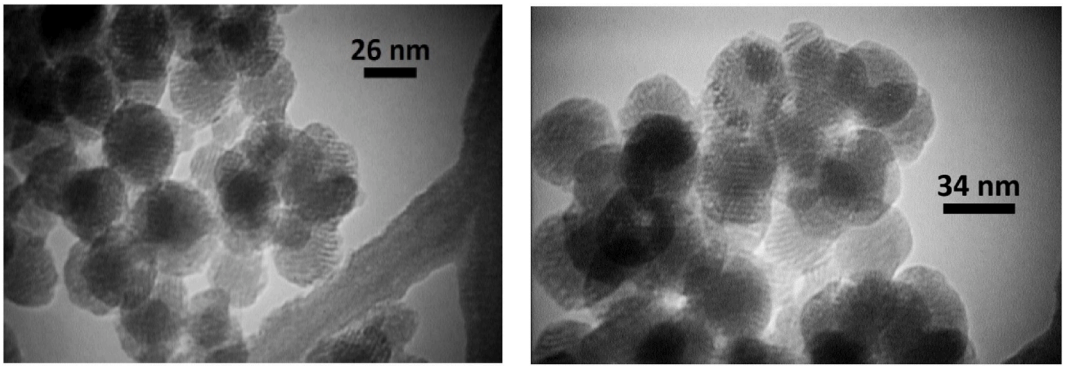

Fig. 7. (A) TEM images of MSN.

SEM images were taken to assess the morphology of MSN and MSN-BA (Fig. 6A–C), as shown in the figures, MSN has particles of a similar size and uniform distribution. MSN-BA (Fig. 6 B&C), as shown in the figures, MSN has particles of similar size and uniform distribution. Particles were synthesized through controlled-size techniques, and observing uniform particles was a result of this synthetic strategy.

TEM was conducted to confirm a more acute estimation of sizes and porous structure (Fig. 7). TEM images showed that MSN was well-ordered with high porosity, and particles have sizes around 30 nm.

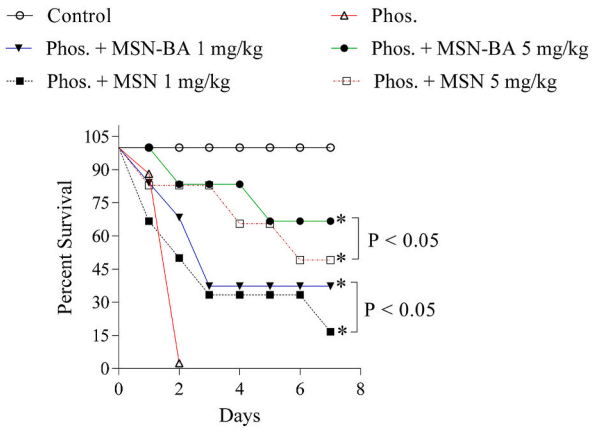

Fig. 8. The MSN and MSN-BA effects on Phos mortality. Rats were treated with a single dose of zinc phosphide (40 mg/kg, gavage), and their survival was monitored for seven days.
MSN: Mesoporous silica nanoparticles
* Significant difference compared to phos-treated rats ($P < 0.001$).

5.2. In vivo study

In vivo studies were performed to determine the ability of MSN to adsorb phosphine gas in an animal model of phosphine poisoning, using two series of rats divided into six groups as described in the Methods section. The zinc phosphide (Phos) poisoned animals received a highly toxic dose of this compound (40 mg/kg); four groups of animals were treated with MSN and MSN-BA at two doses (1 and 5 mg/kg); the first series of animals were observed for seven repeated days and their survival rates were recorded (Fig. 8). The results show that all animals in the control group were alive, whereas all in the Phos-poisoned mice died after less than 48 h, while MSN-BA-treated mice survived to some extent. The survival rate for recipient groups of MSN and MSN-BA in low doses (1 mg/kg) was 15 % for MSN and 35 % for MSN-BA (Fig. 8). By increasing the dose of MSNs to 5 mg/kg, the survival rate was reached up to 70 % for MSN-BA and around 50 % for MSN (Fig. 8). The survival rate for MSN-BA was significantly higher than that of MSN-treated animals. These data indicate the survival rate for the equivalent doses of MSN and MSN-BA was higher for boric acid-functionalized MSN in the current study (Fig. 8). Hence, we could conclude that MSN-BA is a more potent antidote than MSN (Fig. 8).

The second series of animals had their blood samples analysed to determine the possible changes in serum biomarkers due to organ injury; biomarkers, including ALT, AST, LDH, and CKMB were measured, and the corresponding plots are shown in Fig. 9 A-D. Analysis showed that biomarkers of organ injury were significantly reduced in the MSN-treated groups compared to the Phos. group, indicating

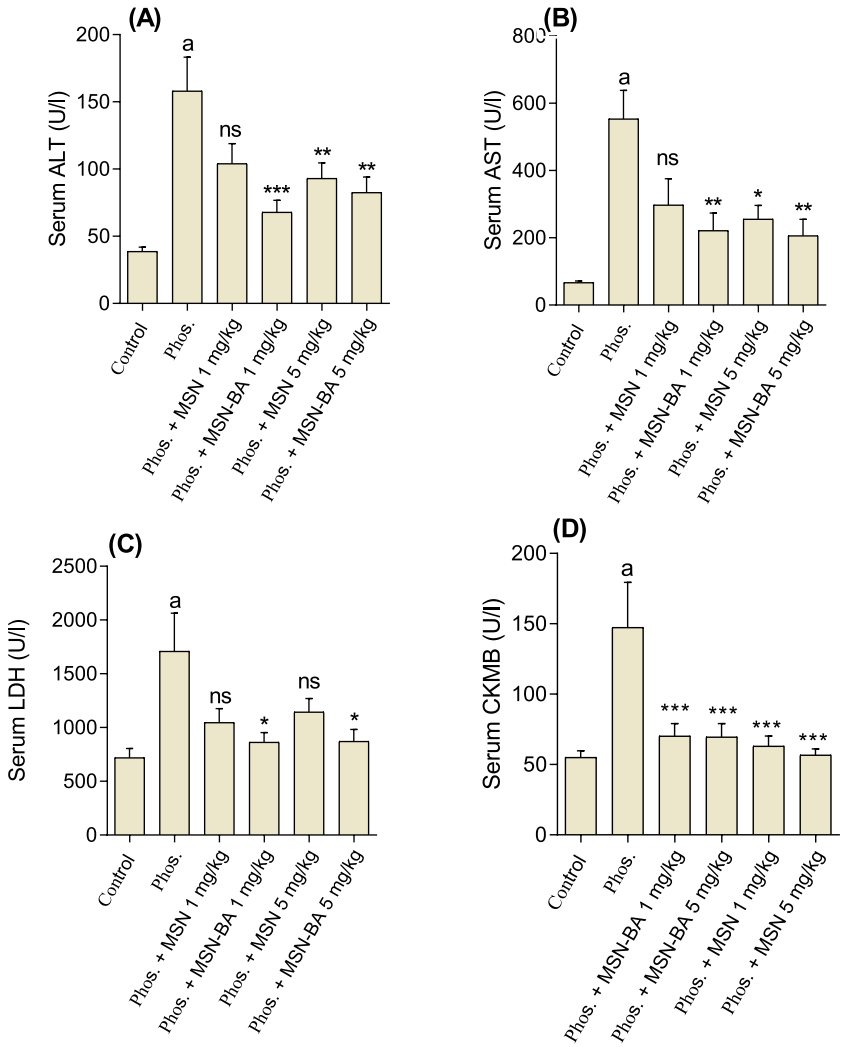

Fig. 9. Serum biochemical measurements in zinc phosphide-treated rats. Animals were treated with Phos (40 mg/kg). MSNs were administered 2 h after Phos poisoning. Serum biomarkers of organ injury were monitored 24 h after Phos intoxication. Measered factors including ALT (A), AST(B), LDH (C), and CKMB (D) are depicted.
Data are represented as mean ± SD (n = 6). [a] Significant difference compared to the control group ($P < 0.01$). Asterisks indicate significant difference as compared with the Phos-treated group (*$P < 0.05$, **$P < 0.01$, and ***$P < 0.001$) ns: Not significant as compared with the Phos-treated group.

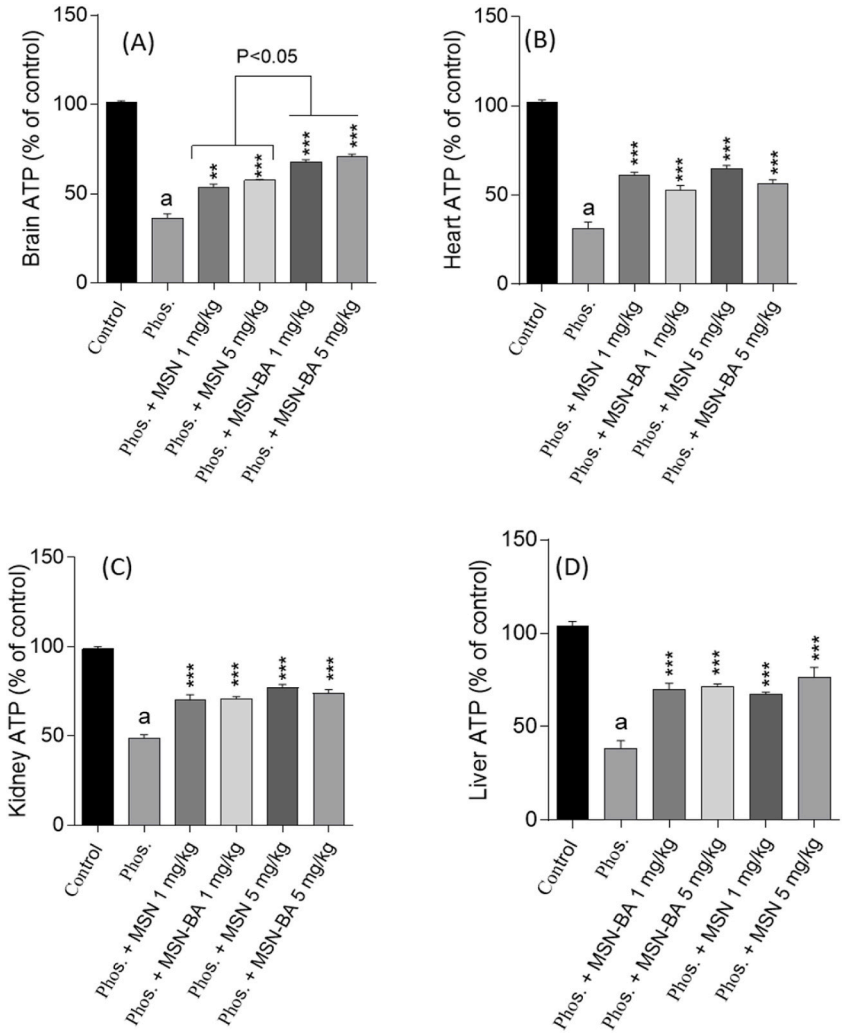

Fig. 10. Heart (A), brain tissue (B), Kidney (C), and Liver (D), ATP levels in Phos-intoxicated rats.
Data are represented as mean ± SD (n = 6). [a] Indicates significantly different as compared with the control group ($P < 0.01$). Asterisks indicate significant difference as compared with the Phos-treated group (*$P < 0.05$, **$P < 0.01$, and ***$P < 0.001$).

that MSN-BA (5 mg/kg) was more effective in inhibiting organ injury.

Tissue ATP levels were measured in different organs like the brain, kidney, heart, and liver (Fig. 10A–D). In Phos. poisoned group the ATP levels in several organ tissues were dropped due to disfunction of cells mitochondria. In Phos-treated animals. Furthermore, in MSN and MSN-BA (1 and 5 mg/kg) treated groups, the ATP content was higher than Phos. Group. (Fig. 10A–D).

6. Discussion

In recent years, MSNs have found their way into biomedicine and nanomedicine. Predictably, MSNs surpass all the requirements to be selected as nanoformulations and are widely used as available drugs in the market [44,45]. The high adsorption capacity of such materials is an essential factor in their pharmaceutical applications, and we've coined a new term for using MSNs as an antidote. This means that MSNs could be recruited as an adsorbent or antidote for some life-threatening intoxications with mineral or organic toxins when administered orally or to humans, a claim supported by several *in vivo* experiments [20,21,23].

In this paper, bare MS nanoparticles (MSN) and boric acid-functionalized MSN (MSN-BA) were synthesized and utilized as an antidote to zinc phosphide-induced toxicity. MSN was prepared using a controlled-size synthesis technique [20] and reacted with boric acid to prepare (MSN-BA). FT-IR spectroscopy showed the successful formation of MSN and the addition of the characteristic bands of Si-OB in MSN-BA. Low-angle XRD showed the distinctive band of MSN crystallinity at 2.5° 2theta, and wide-angle XRD showed the broad bands at 10° and 25° 2theta, indicating SiO_2 amorphous nature. Textural features were determined through N_2 adsorption/-desorption by recruitment of the BET method for surface area analysis and BJH for pore size and volume. A high surface area of around 1025 m^2/g was obtained for MSN by the BJH method, which was reduced to 650 m^2/g in MSN-BA. The morphological study of MSNs

by recording images with SEM and TEM showed the formation of fine MSNs with uniform sizes around 30 nm and well-ordered honeycomb porosity particles that were spherical and very well dispersed in aqueous media. Metal phosphide poisoning has the highest mortality rate of any toxic element in Asian countries such as Iran. The toxicity results from the release of a highly toxic phosphine gas, which shocks vital organs such as the heart and brain, causing the patient to lose consciousness. The lack of a definitive antidote to this poisoning and the inaccessibility of advanced care centers are two significant causes of mortality. We recently introduced a novel antidote agent, sevelamer, to treat ALP poisoning [35].

In 2013, Soltani et al. proposed that boric acid could be an antidote to phosphine. The hypothesis was based on the affinity between phosphorous and boron atoms. The chemical reaction between boric acid and phosphine indicates boric acid is an antidote for phosphine poisoning [46]. The *in vivo* experiment also showed that boric acid could be a new antidote for ALP poisoning [47].

Management of Phos poisoning was reported in several studies in humans by the administration of Thioguma as a hepatoprotective agent [48], a repetitive dose of castor oil [49], and tranexamic acid as antifibrolytic agents [50].

Continuing our previous efforts in utilizing MS materials to manage toxicities, in this work, MSN-BA is introduced as an antidote for phosphine poisoning. Experiments on rats were performed to show MSN and MSN-BA's effectiveness in treating zinc phosphide-poisoned models. The survival rate showed that both MSN and MSN–BA in a 5 mg/kg dose could reduce mortality risk in poisoned animals, and MSN-BA acts more efficiently (Fig. 8). Assessment of organ injury biomarker levels showed that a higher dose of MSN-BA (5 mg/kg) could alleviate injury symptoms. According to the proposed mechanism in Fig. 1, MSN-BA can react with phosphine to form MSN-BA-Phos, an inert compound that small-sized MSNs can be excreted *via* urine, as shown in previous studies by He et al. [51].

7. Conclusion

In this work, MSNs were prepared through a controlled size synthesis technique and applied as an adsorbent of phosphine gas released in rice tablet poisoning in the *in vivo* assessment. Two types of MSNs were synthesized: bare and functionalized with boric acid. Routine characterization experiments such as FT-IR showed that MSN and MSN-BA had desired functional groups. The measurement of textural parameters showed that MSN-BA has less surface area than MSN due to functionalization with boric acid. MSN and MSN-BA could act as an antidote to phosphine gas poisoning. Two sets of *in vivo* experiments, including survival percentage and serum biomarker analysis, were conducted to show that MSN could be applied as a treatment for Phos-induced poisoning. Survival percentage showed that Phos-poisoned animals survived when treated with MSN and MSN-BA. Analysis of serum biomarkers of organ injury showed that MSN-BA could act more efficiently in lowering the symptoms of organ injury in phosphine-poisoned animals. Altogether, MSN could potentially be considered an antidote agent in treating phosphine poisoning. Finally, it is suggested that boric acid functionalized MSN compounds with high reactivity with phosphine gas can be regarded as potential antidote in poisoning.

Declaration

The animals were treated following the instructions approved by the local ethics committee of SUMS in the project with this Ethical Code: IR.SUMS.REC.1395.S823.

CRediT authorship contribution statement

Fatemeh Farjadian: Writing – review & editing, Writing – original draft, Visualization, Validation, Supervision, Software, Resources, Project administration, Methodology, Investigation, Funding acquisition, Formal analysis, Data curation, Conceptualization. **Reza Heidari:** Writing – original draft, Validation, Software, Methodology, Formal analysis, Data curation, Conceptualization. **Soliman Mohammadi-Samani:** Writing – original draft, Investigation, Conceptualization.

Declaration of competing interest

The authors declare that they have no known competing financial interests or personal relationships that could have appeared to influence the work reported in this paper.

Acknowledgment

Fatemeh Farjadian, as the principal investigator and the Grant holder of this project, would like to thank the Vice Chancellor of Research and Technology of SUMS for supporting this project (Grant. No.95-01-36-12883/9906).

References

[1] F. Farjadian, et al., Nanopharmaceuticals and nanomedicines currently on the market: challenges and opportunities, Nanomedicine 14 (1) (2019) 93–126.
[2] M. Hosseini, F. Farjadian, A.S.H. Makhlouf, Smart stimuli-responsive nano-sized hosts for drug delivery, Industrial applications for intelligent polymers and coatings (2016) 1–26.
[3] M. Hoseini-Ghahfarokhi, et al., Applications of graphene and graphene oxide in Smart drug/Gene delivery: is the World Still Flat? Int. J. Nanomed. 15 (2020) 9469.
[4] D. Neha, et al., Metallic nanoparticles as drug delivery system for the treatment of cancer, Expert Opin Drug Deliv 18 (9) (2021) 1261–1290.

[5] F. Farjadian, et al., Mesoporous silica nanoparticles: synthesis, pharmaceutical applications, biodistribution, and biosafety assessment, Chem. Eng. J. 359 (2019) 684–705.
[6] R.K. Kankala, et al., Nanoarchitectured structure and surface Biofunctionality of mesoporous silica nanoparticles, Adv. Mater. 32 (23) (2020) 1907035.
[7] F. Farjadian, et al., Phosphinite-functionalized silica and hexagonal mesoporous silica containing palladium nanoparticles in Heck coupling reaction: synthesis, characterization, and catalytic activity, RSC advances 5 (97) (2015) 79976–79987.
[8] B.M. Al-Shehri, et al., A review: the utilization of mesoporous materials in wastewater treatment, Mater. Res. Express 6 (12) (2019) 122002.
[9] A. Ostovan, et al., Greenificated molecularly imprinted materials for advanced applications, Adv Mater 34 (42) (2022) e2203154.
[10] F. Farjadian, et al., A novel approach to the application of hexagonal mesoporous silica in solid-phase extraction of drugs, Heliyon 4 (11) (2018).
[11] M. Arabi, et al., Hydrophilic molecularly imprinted nanospheres for the extraction of rhodamine B followed by HPLC analysis: a green approach and hazardous waste elimination, Talanta 215 (2020) 120933.
[12] M. Parra, et al., Mesoporous silica nanoparticles in chemical detection: from small species to large bio-molecules, Sensors 22 (1) (2021) 261.
[13] C. Zhang, et al., Applications and biocompatibility of mesoporous silica nanocarriers in the field of medicine, Front. Pharmacol. 13 (2022) 829796.
[14] R.K. Kankala, et al., Ultrasmall platinum nanoparticles enable deep tumor penetration and synergistic therapeutic abilities through free radical species-assisted catalysis to combat cancer multidrug resistance, Chem. Eng. J. 383 (2020) 123138.
[15] M. Akbarian, et al., Theranostic mesoporous silica nanoparticles made of multi-nuclear gold or carbon quantum dots particles serving as pH responsive drug delivery system, Microporous Mesoporous Mater. 329 (2022) 111512.
[16] F. Farjadian, et al., Glucosamine-modified mesoporous silica-coated magnetic nanoparticles: a "Raisin-Cake"-like structure as an efficient theranostic platform for targeted methotrexate delivery, Pharmaceutics 15 (10) (2023) 2491.
[17] K. Zarkesh, et al., Theranostic hyaluronan coated EDTA modified magnetic mesoporous silica nanoparticles for targeted delivery of cisplatin, J. Drug Deliv. Sci. Technol. 77 (2022) 103903.
[18] E. Da'na, Adsorption of heavy metals on functionalized-mesoporous silica: a review, Microporous Mesoporous Mater. 247 (2017) 145–157.
[19] J.O. Tella, J.A. Adekoya, K.O. Ajanaku, Mesoporous silica nanocarriers as drug delivery systems for anti-tubercular agents: a review, R. Soc. Open Sci. 9 (6) (2022) 220013.
[20] F. Farjadian, et al., Controlled size synthesis and application of nanosphere MCM-41 as potent adsorber of drugs: a novel approach to new antidote agent for intoxication, Microporous Mesoporous Mater. 213 (2015) 30–39.
[21] F. Farjadian, et al., In vitro and in vivo assessment of EDTA-modified silica nano-spheres with supreme capacity of iron capture as a novel antidote agent, Nanomed. Nanotechnol. Biol. Med. 13 (2) (2017) 745–753.
[22] E.R. Taqanaki, et al., EDTA-modified mesoporous silica as supra adsorbent of copper ions with novel approach as an antidote agent in copper toxicity, Int. J. Nanomed. 14 (2019) 7781.
[23] H. Mohammadi, et al., In vitro and in vivo evaluation of succinic acid-substituted mesoporous silica for ammonia adsorption: potential application in the management of hepatic encephalopathy, Int. J. Nanomed. 15 (2020) 10085.
[24] W. Zhao, et al., Thiol-functionalized mesoporous silica for effective Trap of mercury in rats, J. Nanomater. 2016 (2016) 9758264.
[25] H. Javdani, et al., Tannic acid-templated mesoporous silica nanoparticles as an effective treatment in acute ferrous sulfate poisoning, Microporous Mesoporous Mater. 307 (2020) 110486.
[26] H. Amiri, et al., Rice tablet: an overview to common material in Iran, Journal of Research in Clinical Medicine 4 (2) (2016) 77–81.
[27] G.S. Bumbrah, et al., Phosphide poisoning: a review of literature, Forensic Sci. Int. 214 (1–3) (2012) 1–6.
[28] A. Ghodsi, B. Dadpour, Z. Shokri Toroghi, Aluminum phosphide poisoning, an unusual presentation, Journal of Basic Research in Medical Sciences 7 (3) (2020) 71–74.
[29] A. Mathai, M.S. Bhanu, Acute aluminium phosphide poisoning: can we predict mortality? Indian J. Anaesth. 54 (4) (2010) 302–307.
[30] A. Juárez-Martínez, et al., Zinc phosphide poisoning: from A to Z, Toxics 11 (7) (2023) 555.
[31] S. Chugh, et al., Adrenocortical involvement in aluminium phosphide poisoning, The Indian journal of medical research 90 (1989) 289–294.
[32] R. Anand, et al., Effect of acute aluminum phosphide exposure on rats—a biochemical and histological correlation, Toxicol. Lett. 215 (1) (2012) 62–69.
[33] A. Karimani, et al., Antidotes for aluminum phosphide poisoning – an update, Toxicol Rep 5 (2018) 1053–1059.
[34] H. Niknahad, et al., Antidotal effect of dihydroxyacetone against phosphine poisoning in mice, J. Biochem. Mol. Toxicol. 35 (11) (2021) e22897.
[35] R. Heidari, et al., Repurposing of sevelamer as a novel antidote against aluminum phosphide poisoning: an in vivo evaluation, Heliyon 9 (4) (2023).
[36] R. Heidari, et al., Mesoporous silica application as an antidote of methotrexate and evaluation of the long-term oral administration: in vitro and in vivo study, J. Mater. Res. (2023) 1–13.
[37] H. Niknahad, et al., Ammonia-induced mitochondrial dysfunction and energy metabolism disturbances in isolated brain and liver mitochondria, and the effect of taurine administration: relevance to hepatic encephalopathy treatment, Clin. Exp. Hepatol. 3 (1) (2017).
[38] R. Heidari, et al., Mitochondrial dysfunction and oxidative stress are involved in the mechanism of methotrexate-induced renal injury and electrolytes imbalance, Biomedicine & Pharmacotherapy = Biomedecine & Pharmacotherapie 107 (2018) 834–840.
[39] R. Heidari, et al., The nephroprotective properties of taurine in colistin-treated mice is mediated through the regulation of mitochondrial function and mitigation of oxidative stress, Biomedicine & Pharmacotherapy = Biomedecine & Pharmacotherapie 109 (2019) 103–111.
[40] Q. Wang, et al., Preparation and properties of borosiloxane gels, J. Appl. Polym. Sci. 99 (3) (2006) 719–724.
[41] M. Soltani, et al., Proposing boric acid as an antidote for aluminium phosphide poisoning by investigation of the chemical reaction between boric acid and phosphine, J. Med. Hypotheses Ideas 7 (1) (2013) 21–24.
[42] C. Huber, et al., Boric acid: a high potential candidate for thermochemical energy storage, Energies 12 (6) (2019) 1086.
[43] A. Khalafi-Nezhad, et al., Silica boron–sulfuric acid nanoparticles (SBSANs): preparation, characterization and their catalytic application in the Ritter reaction for the synthesis of amide derivatives, J. Mater. Chem. 21 (34) (2011) 12842–12851.
[44] F. Farjadian, S. Ghasemi, M. Akbarian, M. Hoseini-Ghahfarokhi, M. Moghoofei, M. Doroudian, Physically stimulus-responsive nanoparticles for therapy and diagnosis, Frontiers in Chemistry 10 (2022) 952675.
[45] C.A. McCarthy, et al., Mesoporous silica formulation strategies for drug dissolution enhancement: a review, Expet Opin. Drug Deliv. 13 (1) (2016) 93–108.
[46] M. Soltani, S.F. Shetab-Boushehri, S.V. Shetab-Boushehri, Chemical reaction between boric acid and phosphine indicates boric acid as an antidote for aluminium phosphide poisoning, Sultan Qaboos Univ Med J 16 (3) (2016) e303–e309.
[47] O.A.H. Sweilum, F.S. Kandeel, D.A.R. Noya, Management of acute aluminum phosphide toxicity in rat model with a novel intervention, a trial of boric acid, The Egyptian Journal of Forensic Sciences and Applied Toxicology 17 (2) (2017) 57–72.
[48] G. Bilics, et al., Successful management of zinc phosphide poisoning—a Hungarian case, Int. J. Emerg. Med. 13 (1) (2020) 48.
[49] V. Shakoori, et al., Successful management of zinc phosphide poisoning, Indian J. Crit. Care Med.: Peer-reviewed, Official Publication of Indian Society of Critical Care Medicine 20 (6) (2016) 368.
[50] A.R.M. El Naggar, N.M. El Mahdy, Zinc phosphide toxicity with a trial of tranexamic acid in its management, J. Adv. Res. 2 (2) (2011) 149–156.
[51] Q. He, et al., In vivo biodistribution and urinary excretion of mesoporous silica nanoparticles: effects of particle size and PEGylation, Small 7 (2) (2011) 271–280.